Supplementary information

Small-molecule inhibition of a depalmitoylase enhances *Toxoplasma* host-cell invasion

Matthew A. Child[1], Carolyn I. Hall[2], Josh R. Beck[3], Leslie O. Ofori[1], Victoria E. Albrow[1], Megan Garland[1], Paul W. Bowyer[1], Peter J. Bradley[3], James C. Powers[4], John C. Boothroyd[2], Eranthie Weerapana[5] and Matthew Bogyo[1,2]

Departments of [1]Pathology, [2]Microbiology and Immunology Stanford University School of Medicine, Stanford, CA, 94305 USA

[3]Department of Microbiology, Immunology and Molecular Genetics, University of California, Los Angeles, Los Angeles, California, USA

[4]Department of Chemistry, Georgia Institute of Technology, Atlanta, GA USA.

[5]Department of Chemistry, Boston College, Chestnut Hill, Massachusetts 02467, USA.

* Correspondence: mbogyo@stanford.edu

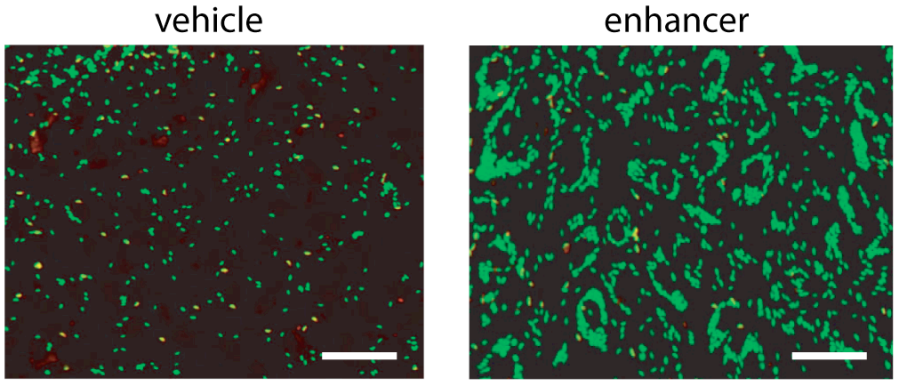

Supplementary figure 1. In the original high-throughput screening conditions substituted chloroisocoumarins dramatically enhance invasion of host-cells. Representative images for attachment/invasion assays using GFP-parasites (green particles) following a single 50 μM treatment of JCP174 (enhancer) or DMSO (vehicle) using the red/green assay described in the methods section (Yellow particles indicate GFP parasites labeled with an antibody conjugated to an alexafluor594 fluorophore). Scale bar, 100 μm.

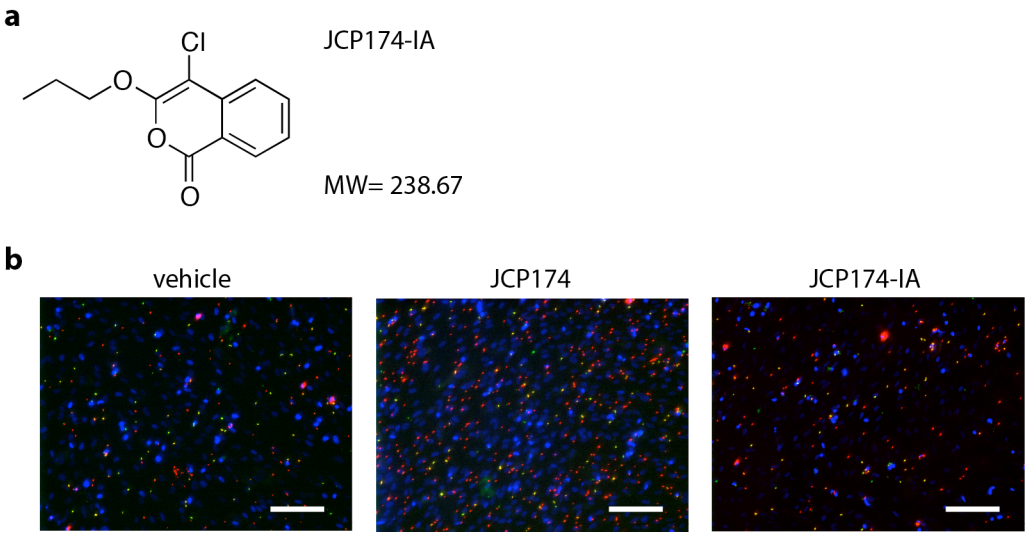

Supplementary figure 2. Enhancer compounds are dependent upon the aromatic amine in the 7-substituent position for activity. a, Structure of the inactive JCP174 analogue (JCP174-IA). **b,** Representative images for attachment/invasion assays using RFP-parasites following a single 50 μM treatment of JCP174, JCP174-IA or DMSO (vehicle) using the red/green assay described in the methods section. Blue = DAPI stained host-cell nuclei; Red = RFP expressing tachyzoites; Yellow = RFP expressing tachyzoites labeled with an antibody conjugated to an alexa488 fluorophore. Scale bar, 100 μm.

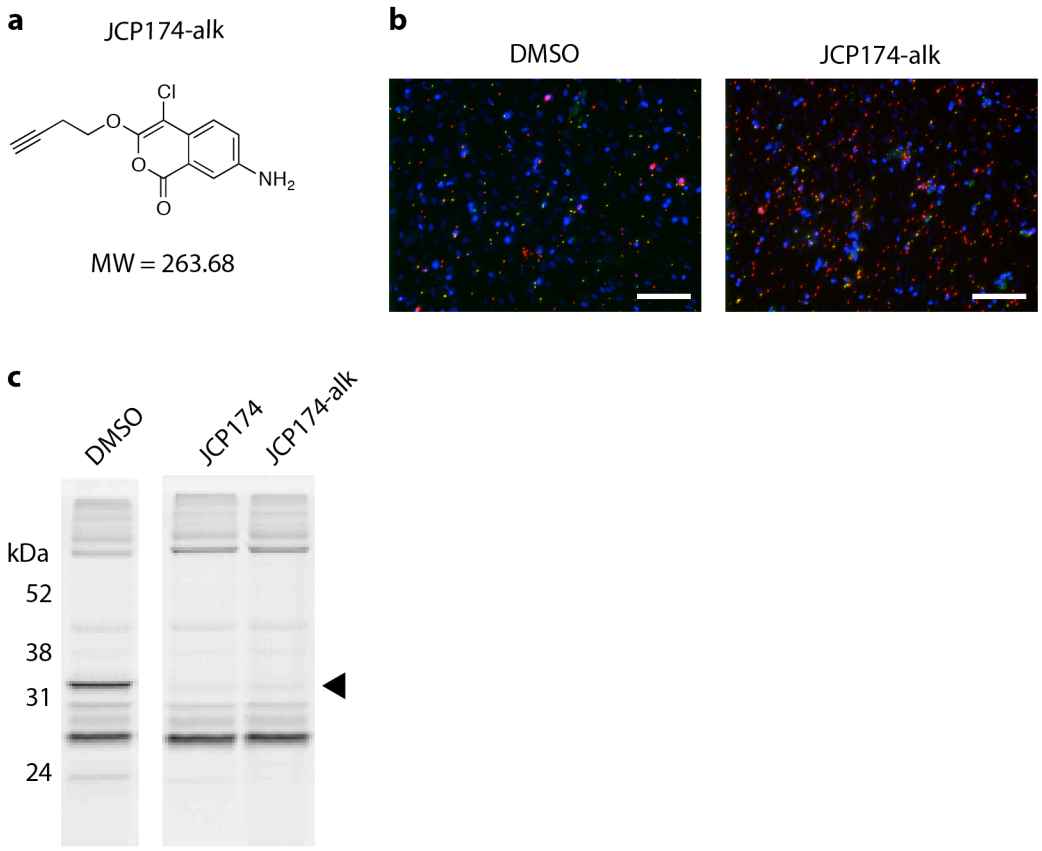

Supplementary figure 3. JCP174-alkyne behaves the same as the unmodified parent compound. a, Structure of JCP174-alkyne (JCP174-alk). **b,** Representative images for attachment/invasion assays using RFP-parasites with a single 50 µM treatment of JCP174-alk or DMSO (vehicle) using the red/green assay described in the methods section. Blue = DAPI stained host-cell nuclei; Red = RFP expressing tachyzoites; Yellow = RFP expressing tachyzoites labeled with an antibody conjugated to an alexa488 fluorophore. Scale bar, 100 µm. **c,** Activity-based probe (ABP) competition assays of FP-rhodamine labeled serine hydrolase targets in tachyzoites lysates comparing JCP174-alk to DMSO (control) and JCP174 (parent compound). Arrowhead indicates principal target of competition.

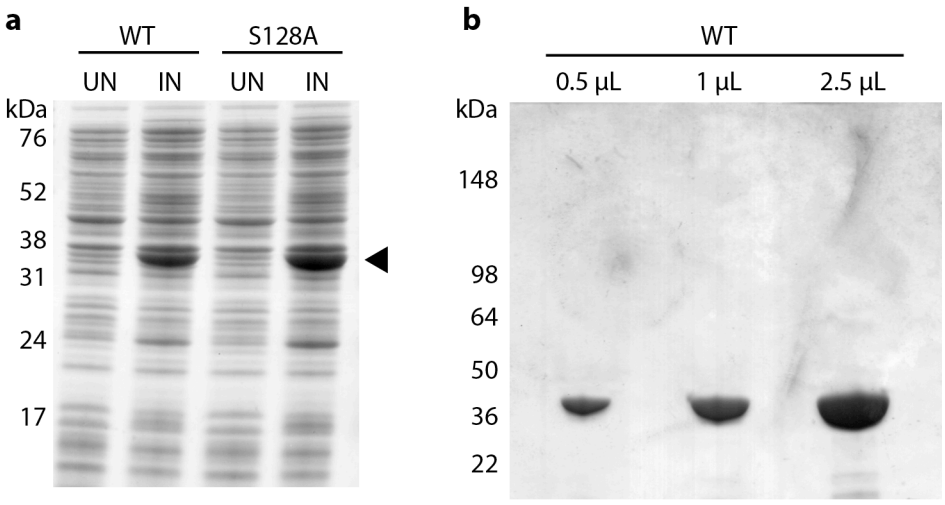

Supplementary figure 4. TgPPT1$_{WT}$ and TgPPT1$_{S128A}$ can be expressed and purified from *E. coli.* **a,** Coomassie stained SDS-PAGE gel of uninduced (UN) and induced (IN) samples from an *E. coli* expression culture for TgPPT1$_{WT}$ and TgPPT1$_{S128A}$. Arrowhead indicates induced protein species. **b,** Coomassie stained gel of samples taken following a representative purification of TgPPT1$_{WT}$, as described in the methods section.

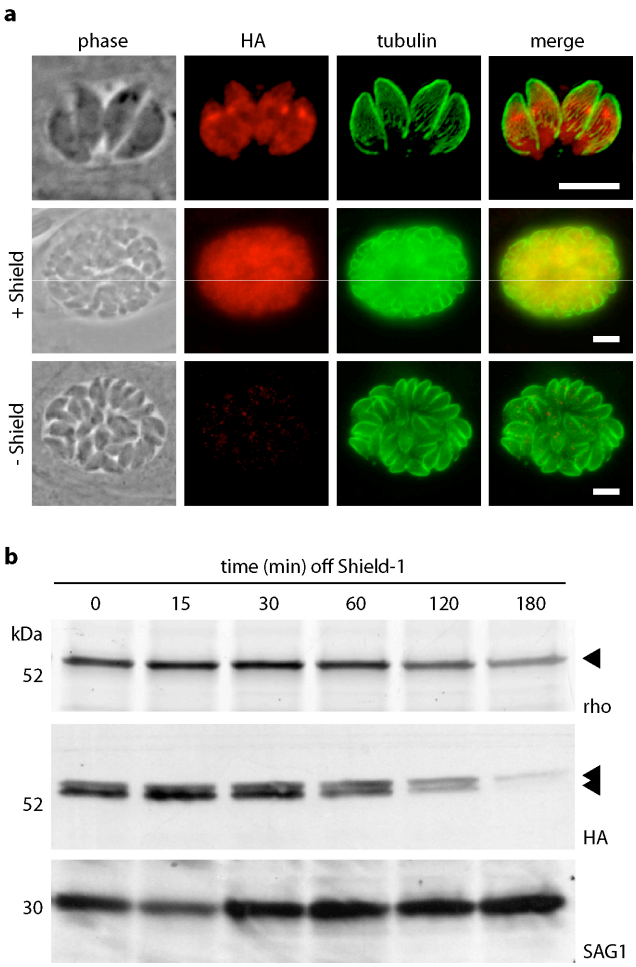

Supplementary figure 5. TgPPT1-HAdd is cytosolically localized and rapidly degraded upon removal of Shield-1. a, Cellular localization of TgPPT1-HAdd by indirect immunofluorescent assay, and conditional knockdown of TgPPT1-HAdd upon removal of Shield-1. HA, anti-HA Ab. tubulin, anti-tubulin Ab. Scale bar, 6 µm. **b**, Timecourse of knock-down of TgPPT1-HAdd upon removal of Shield-1 observed through FP-rhodamine labeling of residual TgPPT1-HAdd activity (rho, top panel with the labeled species indicated by a single arrowhead) and Western blot of total TgPPT1-HAdd protein levels (HA, middle panel). SAG1, loading control. Double arrowhead indicates HA-positive doublet sometimes observed in the HAdd-tagged strain following FP-rhodamine labeling.

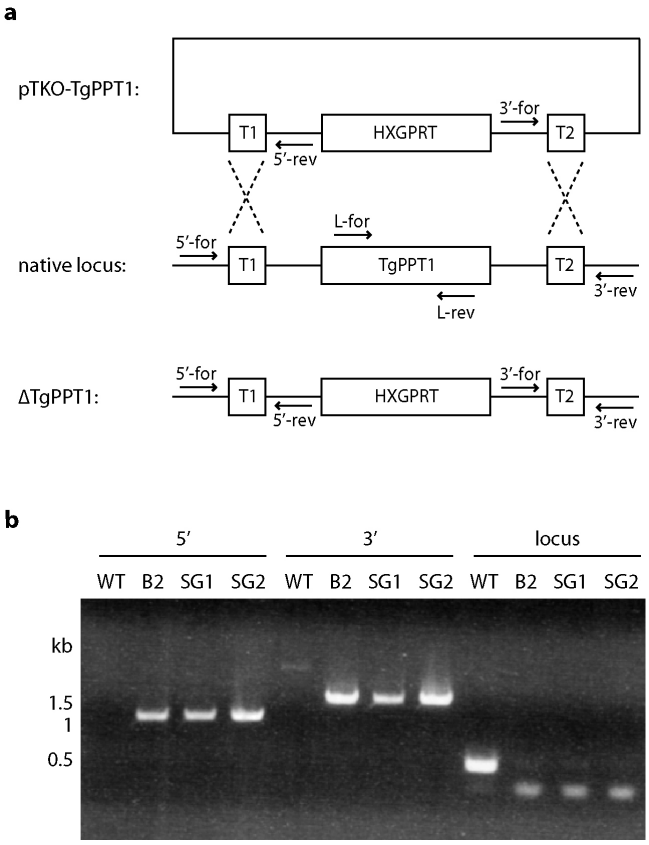

Supplementary figure 6. PCR verification of TgPPT1 knockout. a, Schematic of the knockout plasmid (pTKO-TgPPT1), the native TgPPT1 locus, and the expected genomic rearrangement resulting from double cross-over homologous recombination of pTKO-TgPPT1 with the TgPPT1 locus to generate ΔTgPPT1. Expected points of recombination are indicated with dashed lines. *T1* and *T2*; 5′ and 3′ targeting regions. *HXGPRT;* hypoxanthine-xanthine-guanine phosphoribosyl transferase drug selection cassette. Arrows indicate positions and names of primers used to verify the predicted rearrangment of the TgPPT1 locus. **b**, Three ΔTgPPT1 clones (B2, SG1, SG2) were compared alongside untransfected wild-type (WT) in three different PCR reactions: 5′: integration specific PCR using primers 5′-for and 5′-rev to give an expected PCR product of 1.2 kb. 3′: integration specific PCR using primers 3′-for and 3′-rev to give an expected PCR product of 1.9 kb. locus: PCR to amplify native TgPPT1 locus using primers L-for and L-

rev to give an expected PCR product of 0.4 kb. Clone SG1 was selected and used for all subsequent studies described.

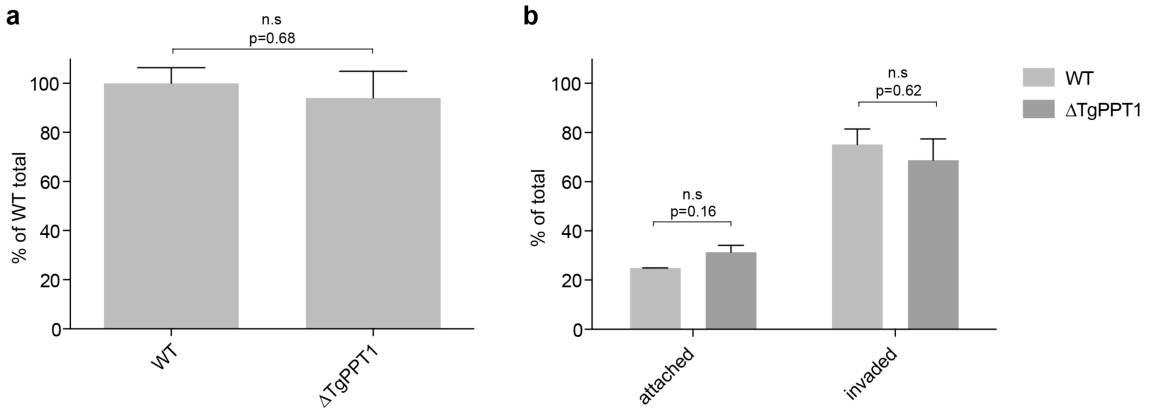

Supplementary figure 7. ΔTgPPT1 parasites are indistinguishable from wild-type in their ability to attach to and invade host cells. Invasion assays were performed using equal numbers of parasites (input = 1 x 10^6 parasites/well). The standard red/green assay was used as described in the methods section. **a**, Total number of parasites (attached plus invaded) relative to wild type for wild-type (WT) and ΔTgPPT1. There is no significant difference between the two strains in terms of the total number of parasites counted (raw mean counts: wild-type total = 2405, SEM +/- 154.4; ΔTgPPT1 total = 2260.9, SEM +/- 261.9). **b**, Fractions of the respective totals counted as attached or invaded plotted as percent of the total number counted for that parasite line. The fraction of the total number of parasites that have attached and invaded is not significantly different for the two parasite lines (raw mean counts: wild-type attached = 599.1, SEM +/- 0.8; wild-type invaded = 1805.9, SEM +/- 153.6; ΔTgPPT1 attached = 707.4, SEM +/- 64.8; ΔTgPPT1

invaded = 1553.5, SEM +/- 197.1). Student's *t*-test; "n.s" indicates no significant difference with the P value shown; means +/- SEM for *n* = 8 experiments.

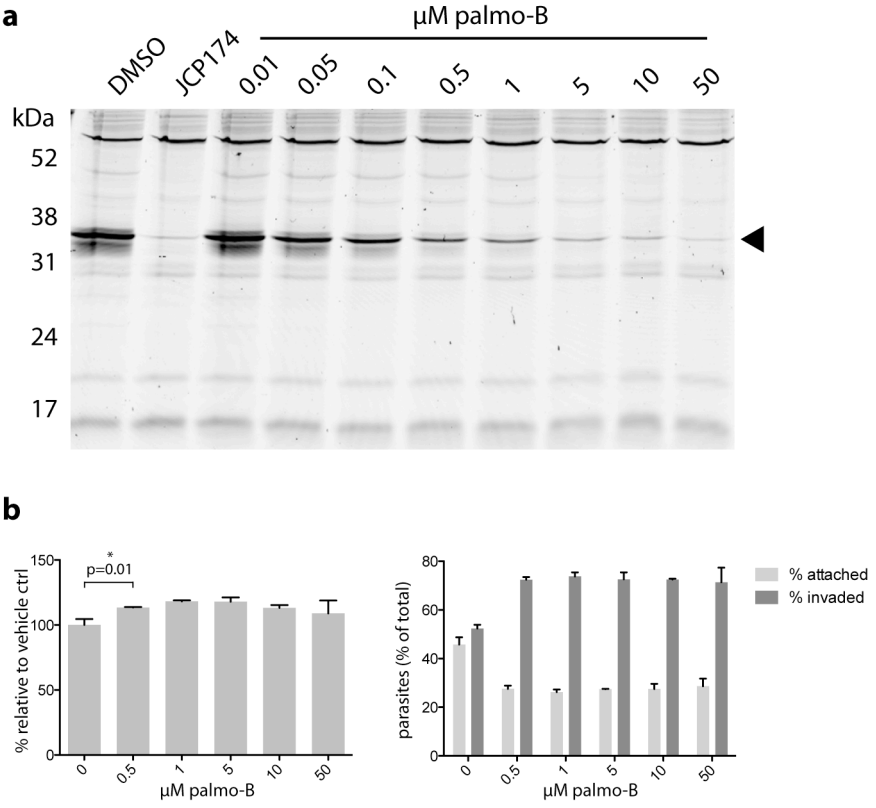

Supplementary figure 8. Palmostatin-B competes for FP-rhodamine labeling of the TgPPT1 species in gel, and enhances invasion of host-cells. a, Activity-based probe (ABP) competition assays of FP-rhodamine labeled serine hydrolase targets in tachyzoite lysates using vehicle (DMSO), 50 µM JCP174 and a titration of palmostatin-B (palmo-B). Arrowhead indicates principal target of competition for JCP174 and palmostatin-B. **b**, Attachment/invasion assays with a titration of palmostatin-B using the red/green assay

described in the methods section. Student's *t*-test; asterisk indicates significance with the P value shown; means +/- SEM for $n = 8$ experiments.

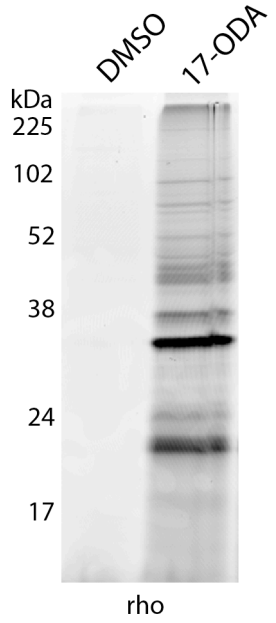

Supplementary figure 9. *Toxoplasma* tachyzoites can be metabolically labeled with 17-octadecynoic acid (17-ODA). SDS-PAGE of azido-rhodamine "Clicked" sample (rho) of the membrane fractions prepared from tachyzoites (RH1) metabolically labeled with DMSO or 17-ODA.

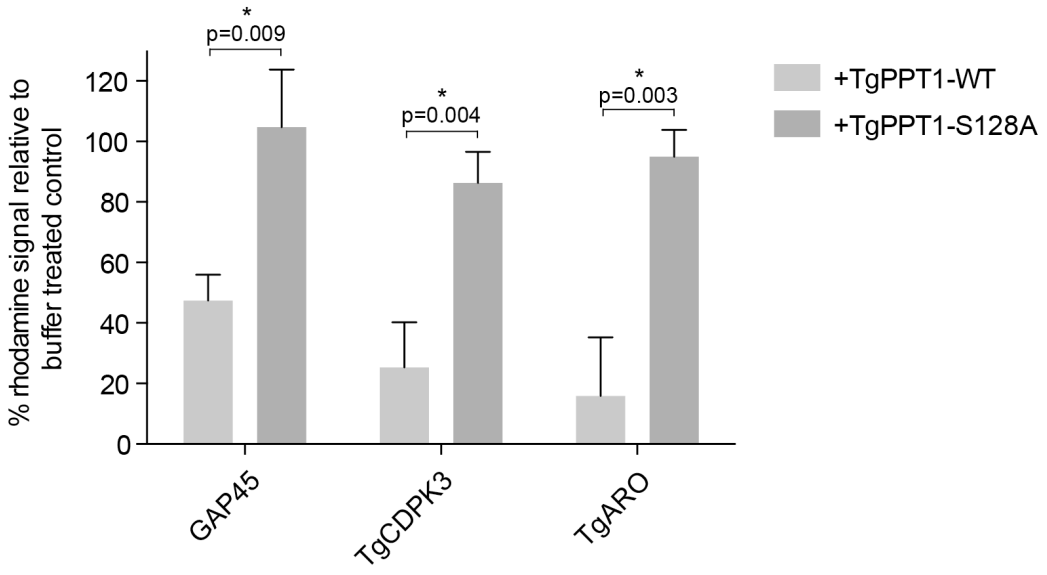

Supplementary figure 10. Normalized residual azido-rhodamine labeling of TgPPT1 substrates following digestion with $TgPPT1_{WT}$ and $TgPPT1_{S128A}$. Western blot signal intensities were normalized to buffer treated control to generate a protein loading normalization factor. The fluorescent signal for the rhodamine labeling of the palmitoylated substrates was measured and adjusted for background signal intensity, and then normalized according protein loading values. The final normalized fluorescence intensity values (representing residual rhodamine labeling of substrates following digestion) were expressed as a percentage of the buffer treated control (100%), and plotted as such for the enzymatic treatments with either $TgPPT1_{WT}$ or $TgPPT1_{S128A}$. Student's *t*-test; asterisk indicates significance with the P value shown; means +/- SD for $n = 3$ independent experiments.

a

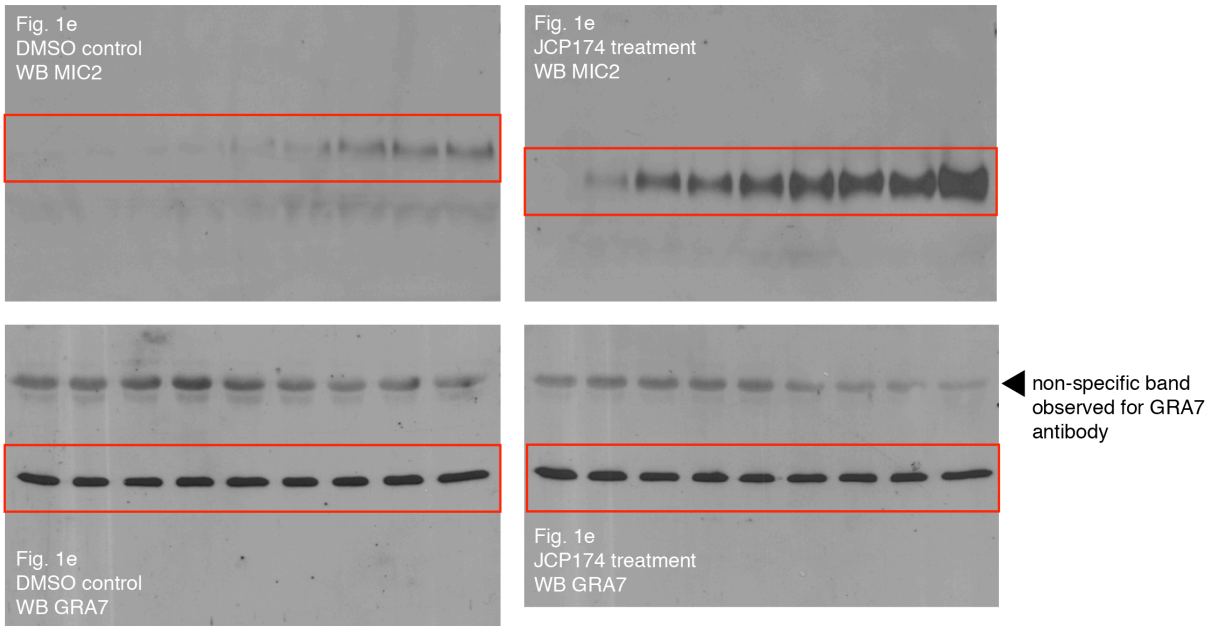
Fig. 1e
DMSO control
WB MIC2
Fig. 1e
JCP174 treatment
WB MIC2
Fig. 1e
DMSO control
WB GRA7
Fig. 1e
JCP174 treatment
WB GRA7
non-specific band
observed for GRA7
antibody

b

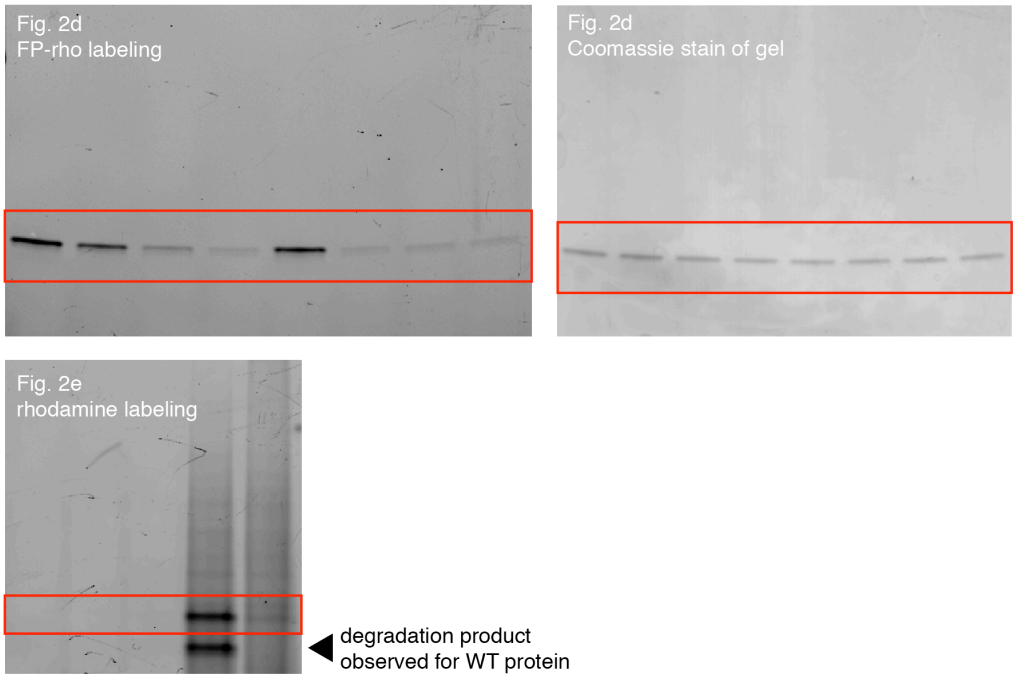
Fig. 2d
FP-rho labeling
Fig. 2d
Coomassie stain of gel
Fig. 2e
rhodamine labeling
degradation product
observed for WT protein

C

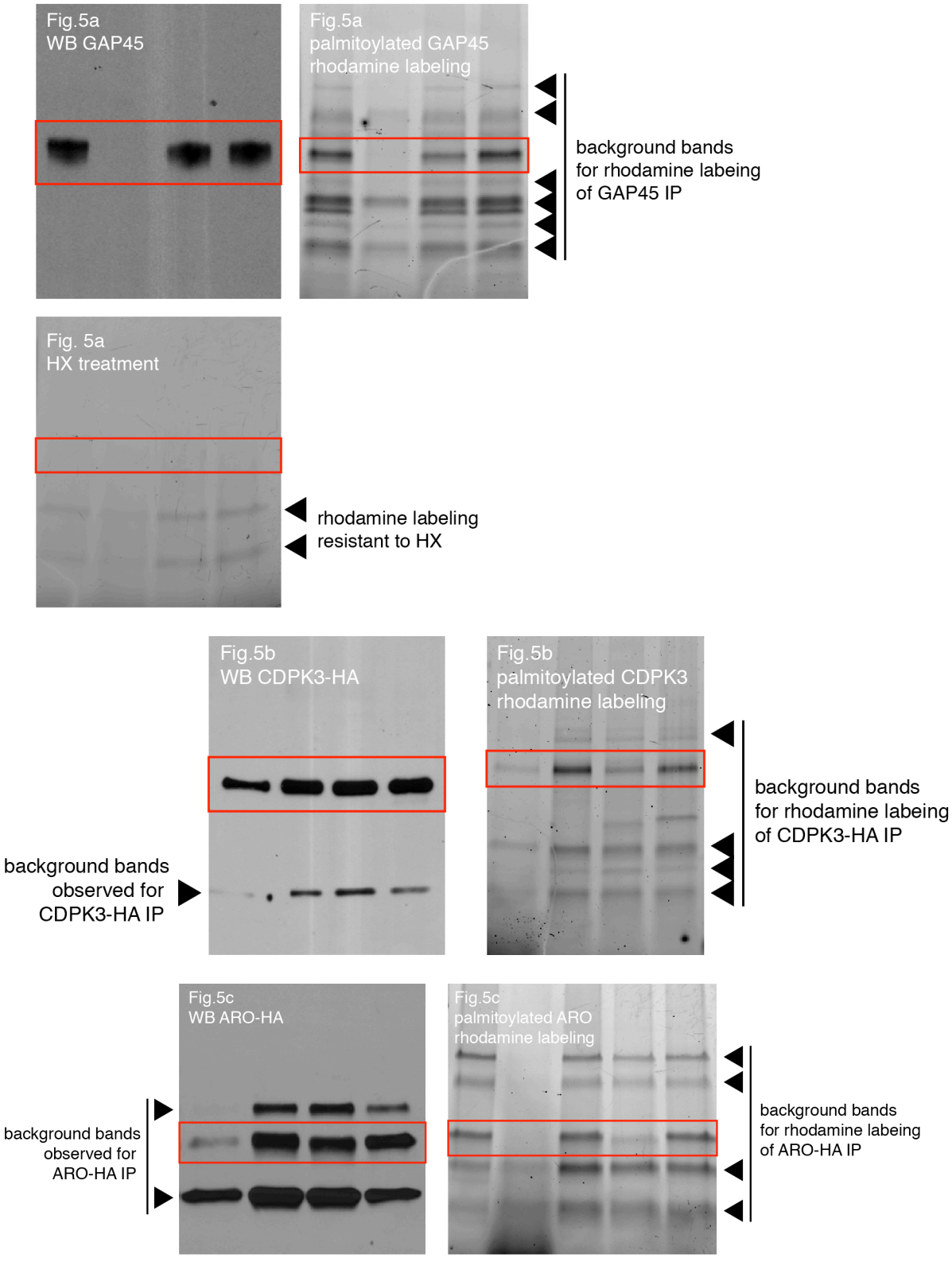
Fig.5a
WB GAP45
Fig.5a
palmitoylated GAP45
rhodamine labeling
background bands
for rhodamine labeing
of GAP45 IP
Fig. 5a
HX treatment
rhodamine labeling
resistant to HX
Fig.5b
WB CDPK3-HA
Fig.5b
palmitoylated CDPK3
rhodamine labeling
background bands
for rhodamine labeing
of CDPK3-HA IP
background bands
observed for
CDPK3-HA IP
Fig.5c
WB ARO-HA
Fig.5c
palmitoylated ARO
rhodamine labeling
background bands
for rhodamine labeing
of ARO-HA IP
background bands
observed for
ARO-HA IP

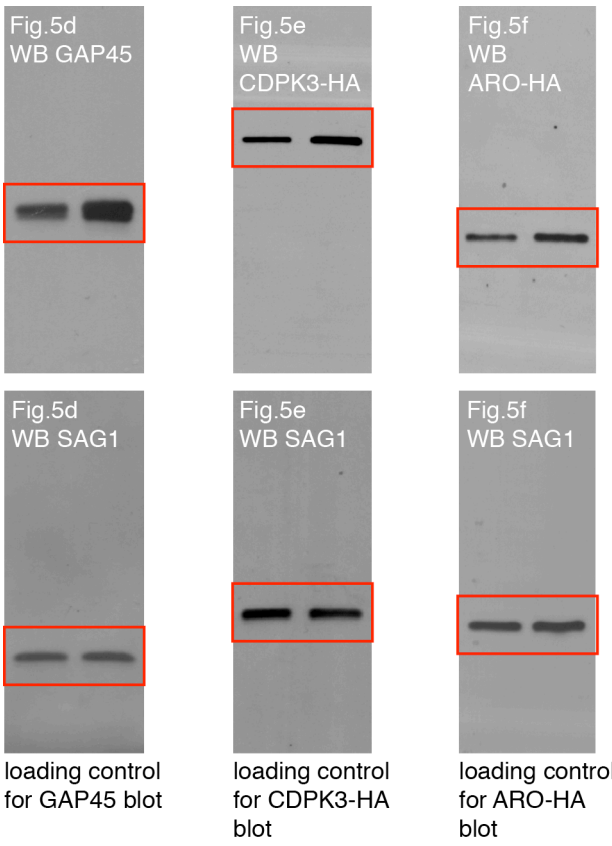

Supplementary figure 11. Full Western blots and fluorescent gel scans. Red boxes indicate regions cropped for main figures. **a**, blots for figure 1e. **b**, coomassie stained gel and fluorescent gel scans for figure 2d and 2e. **c,** blots and fluorescent gel scans for figure 5a-f. Arrowheads indicate non-specific labeling by antibodies or azido-rhodamine following Click reactions.

Supplementary table 1. Combined data for parallel mass-spectrometry target identification approaches. See Excel spreadsheet for data. See Methods section for a description of the triaging approach taken for these preliminary datasets.

Supplementary table 2. Stringent analysis of the MS data identifies TGGT1_083860, a putative phospholipase/carboxylesterase as the principal target of JCP174. See Excel spreadsheet for data.

Supplementary table 3. µM IC50s for compound inhibition of TgPPT1.

compound	µM IC50
JCP174	1.32
JCP174-alk	1.79
JCP174-IA	9280
JCP222	0.59
JCP362	1.24
palmo-B	0.098

Supplementary table 4. DNA Primers.

Primer name	Nucleotide sequence (5´- 3´)
TgPPT1-amplify-FOR	CAATAAGTACATATGGCGTCTCTCCAGCCAGG
TgPPT1-amplify-REV	GTTAAATTTGGATCCTCATCAGTTTGTTGTGAGGACGTTTTCG
TgPPT1-S128A-FOR	CGAATTATCCTCGCAGGATTCGCTCAAGGCGGCGCCCTCGCCTAC
TgPPT1-S128A-REV	GTAGGCGAGGGCGCCGCCTTGAGCGAATCCTGCGAGGATAATTCG
TgPPT1-DD target primer P1	TACTTCCAATCCAATTTAGCTCCAGTCGACACTCCAGC
TgPPT1-DD target primer P2	TCCTCCACTTCCAATTTTAGCGTTTGTTGTGAGGACGTTTTCGATG
TgPPT1-KO 5' target FOR	CGTTTTGCCGGATTCTCGAGATTCCTTTCTTCCCTAAGAGTCC

TgPPT1-KO 5' target REV	GAGAAGCACAGGAATTCGAGCTGGAGTGTCGACTGG
TgPPT1-KO 3' target FOR	CGACGAACAAGCTTAGACAGTCTGCGAAGCTGGAGG
TgPPT1-KO 3' target REV	GTCACGAGGGCCCCACCGCTACAAGTGAACGTGTACACC
TgPPT1 5' integration screen FOR	GAAGTGCTGAAGACTGTATACTGG
TgPPT1 5' integration screen REV	CAATTAACCCTCACTAAAGGGAACAAAAGC
TgPPT1 3' integration screen FOR	CAAGGACGCAGAAAGGAACAAACACCG
TgPPT1 3' integration screen REV	GAACACATGGACAGCGAATGAAGG
TgPPT1-locus check FOR	CCTCGCCTCCAAGCAGCGCATCG
TgPPT1-locus check REV	GCCTCTGCGTAGTGTCGTCTCACG